Coherent x-ray diffraction imaging of paint pigment particles by scanning a phase plate modulator

2011 New J. Phys. 13 103022

(http://iopscience.iop.org/1367-2630/13/10/103022)

New Journal of Physics
The open-access journal for physics

Coherent x-ray diffraction imaging of paint pigment particles by scanning a phase plate modulator

Bo Chen[1,6], Fucai Zhang[2], Felisa Berenguer[1], Richard J Bean[1], Cameron M Kewish[3,7], Joan Vila-Comamala[3,8], Yong S Chu[4], John M Rodenburg[2] and Ian K Robinson[1,5,6]

[1] London Centre for Nanotechnology and Department of Physics and Astronomy, University College London, London WC1H 0AH, UK
[2] Department of Electronic and Electrical Engineering, University of Sheffield, Sheffield S1 3JD, UK
[3] Paul Scherrer Institut, 5232 Villigen PSI, Switzerland
[4] National Light Source II, Brookhaven National Laboratory, Upton, NY 11973, USA
[5] Research Complex, Harwell-Oxford Campus, Didcot, Oxfordshire, OX11 0DE, UK
E-mail: bo.chen2008@ucl.ac.uk and i.robinson@ucl.ac.uk

New Journal of Physics **13** (2011) 103022 (8pp)
Received 21 June 2011
Published 19 October 2011
Online at http://www.njp.org/
doi:10.1088/1367-2630/13/10/103022

Abstract. We have implemented a coherent x-ray diffraction imaging technique that scans a phase plate to modulate wave-fronts of the x-ray beam transmitted by samples. The method was applied to measure a decorative alkyd paint containing iron oxide red pigment particles. By employing an iterative algorithm for wave-front modulation phase retrieval, we obtained an image of the paint sample that shows the distribution of the pigment particles and is consistent with the result obtained from a transmission x-ray microscope. The technique has been experimentally proven to be a feasible coherent x-ray imaging method with about 120 nm spatial resolution and was shown to work well with industrially relevant specimens.

[6] Authors to whom any correspondence should be addressed.
[7] Current address: Synchrotron Soleil, 91192 Gif-sur-Yvette, France.
[8] Current address: Advanced Photon Source, Argonne National Laboratory, Argonne, IL 60439, USA.

Contents

1. Introduction

With the emergence of modern synchrotron x-ray sources, coherent x-ray diffraction imaging has been successfully applied in materials and biological sciences [1–7] since its first demonstration by Miao *et al* [8]. The technique has been improved both experimentally [7, 9, 10] and algorithmically [11–14] in order to circumvent its original limitations, such as the isolated sample requirements under coherent x-ray illumination and the difficulties associated with obtaining a unique image solution by reconstructing a single diffraction pattern of a sample using phase retrieval algorithms.

Here, we present a wave-front modulation coherent x-ray diffraction imaging system [15, 16], which uses a recently developed algorithm for phase retrieval. The method can be applied to extended samples without tight support constraints and provides a unique solution to the phase retrieval process without stagnation. To verify its feasibility, experiments have been performed on an industrial alkyd paint sample. This type of paint is one of the most important varieties of coating in the world [17], and its chemical construction and physical performances have been widely studied for a long time [17–21].

The measured alkyd paint specimen consists of two main components: alkyd resin and iron oxide particles, which act as the film former/binder and pigment of the paint, respectively. The sample is a decorative coating with high-ultraviolet (UV)-resistant capabilities that are generated from the iron oxide particles, whose maximum size is 500 nm according to information provided by the manufacturer. The UV resistance is crucial to the service life of outdoor coatings since, in numerous cases, UV radiation induces most of the chemical and physical breakdown of the substrates and paint coatings themselves [22]. These iron oxide particles are effective absorbers of UV radiation, providing essential protection to the substrates and the alkyd resin and thus ensuring that the cured coating films have a long service life and high color stability. These performances of the paint are dominated by the distribution of iron oxide particles in the alkyd resin. In this paper, we present a practical method of measuring this property, which is the subject of ongoing investigations.

2. Experiment and methods

Figure 1 schematically presents the experimental setup of this imaging method. A phase plate with a known, random pattern is inserted in the x-ray path between the sample and the detector, functioning as a wave-front modulator.

There are three planes perpendicularly intersecting the primary optical axis that are of relevance to this coherent x-ray imaging method: the sample plane, the phase plate/modulator

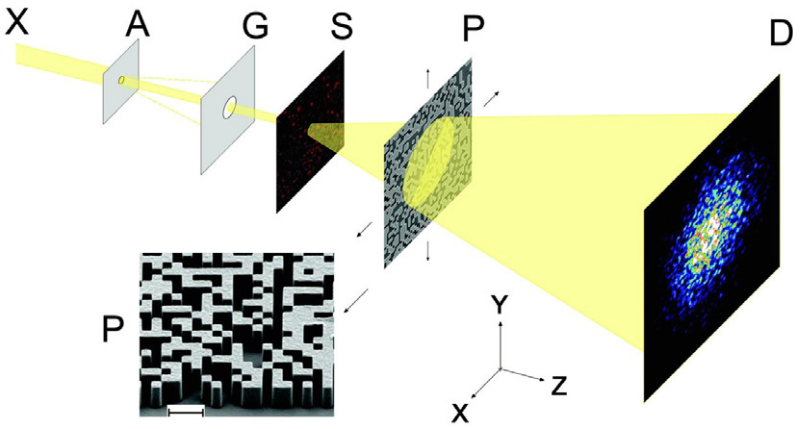

Figure 1. Schematic diagram of the experimental setup. The x-ray beam (X) travels from left to right. A coherent part of the beam is selected by a pinhole aperture (A), and scattering is removed by a guard aperture (G). The sample (S) diffracts the coherent beam, and the wave-fronts are then modulated by a phase plate modulator (P). The detector (D) measures the diffraction patterns in the far-field of the sample. The inset P is a scanning electron micrograph of the nanofabricated phase plate (the scale bar in the inset represents 1 μm).

plane and the detector plane (these planes are labeled as S, P and D, respectively, in figure 1). During the experiment, the phase plate is scanned linearly or circularly in the plane labeled P. At each phase plate position, a diffraction pattern of the same illuminated region of the sample is acquired [15, 16]. An image of the sample is obtained from these diffraction patterns without prior knowledge of the structure of the illuminating x-ray probe. However, the phase distribution function of the phase plate and the parameters of the experiment setup geometry are measured carefully and given as the input to a phase retrieval algorithm. The algorithm uses an iterative calculation that cycles back and forth between the phase plate and the detector planes.

The iterative procedure starts from an original random estimate ψ_n (n is the iteration number, and $n = 0$ here) of the x-ray wave-front before the phase plate and then runs repetitively with the following steps.

(1) Modulate the estimated ψ_n with the phase distribution function of the plate and generate a modulated wave-front ψ'_n.

(2) Propagate the ψ'_n to the detector using a Fourier transform to obtain an estimated diffraction pattern Ψ_n^{d}. Here, the Fourier transform is used because the far-field recording geometry is employed in our experiment. For a near-field recording geometry, the Fresnel propagator can be used instead.

(3) Replace the magnitude of Ψ_n^{d} by the square root of the measured intensity of the diffraction pattern to obtain an updated diffraction pattern of the wave-front $\Psi_n^{\mathrm{d}'}$.

(4) Backpropagate $\Psi_n^{\mathrm{d}'}$ to the phase plate plane using an inverse Fourier transform.

(5) Remove the phase distribution function of the plate to obtain an updated estimate Ψ_{n+1} of the wave-front before the phase plate.

(6) Repeat steps 1–5 at the next phase plate position. If the last plate position was reached, then use the first one again, and the iterative process cycles through the recorded diffraction patterns.

The convergence of the iterative process is monitored by the normalized root-mean-square error [23]. When there is no further improvement of the reconstruction quality, the iteration ends and an exit wave of the object has been generated on the phase plate. Finally, the image of the object is acquired by further backpropagating the wave-front to the sample plane using an angular spectrum algorithm [24].

The experiment was carried out at the cSAXS beamline at the Swiss Light Source on a piece of cured alkyd paint film that was several millimeters wide and about 25 μm thick. The sample had experienced 3 min mechanical agitation before it was applied to a polypropylene substrate. The cured dry sample was then peeled off the substrate as a free-standing film. An x-ray beam from an undulator insertion device was used for the experiment. A double-crystal Si(111) monochromator was used to select x-rays of energy 6.2 keV ($\lambda \approx 2.0$ Å) from the beam. A 10 μm diameter pinhole aperture (labeled as A in figure 1) was installed 183 mm upstream of the sample to select a coherent part of incident beam. A guard aperture (marked G in figure 1) 100 μm in diameter followed the pinhole aperture. It was installed 23 mm upstream of the sample to block scattered x-rays from the pinhole aperture. A random-patterned phase plate was positioned 24 mm downstream from the sample. The plate [25], shown in the inset P of figure 1, comprises a randomly filled grid of $300 \times 300\,\text{nm}^2$ 'pixels' designed to shift the phases of wave-fronts by 0 (empty pixels) or π radians (1.1 μm thick Au pixels) under 6.2 keV x-ray illumination. The phase plate was mounted on a piezoelectric translation stage. The distance between the phase plate and the x-ray detector (a charge-coupled device (CCD) camera from Princeton Instruments, 16 bits cooled, 1:1 optical taper coupling, columnar CsI scintillator and effective pixel size $20 \times 20\,\mu\text{m}^2$) was 7 m to ensure far-field diffraction conditions. During measurements, the phase plate was scanned transversely to the beam by the piezoelectric translation stage linearly or circularly in 600 nm steps, and five diffraction patterns were acquired at different phase plate positions. Each diffraction pattern consisted of the sum of ten accumulated 2 s exposures. The same scan with identical positions of the phase plate was then recorded without a sample in the x-ray path to obtain the structure of the x-ray illumination beam, which was treated to be a background illumination function. This allowed the contributions from the beamline and the sample to be separated.

Full-field x-ray imaging measurements were carried out on the same alkyd paint sample by a transmission x-ray microscope (TXM) at beamline 32-ID-C of the Advanced Photon Source (APS) at the Argonne National Laboratory (ANL) in order to verify the reliability of the coherent x-ray imaging method. The TXM was operated under the Zernike phase contrast mode using an 8.0 keV ($\lambda \approx 1.5$ Å) x-ray source. The incident beam was focused onto the sample by a capillary condenser. The transmitted x-ray beam by the sample was refocused by a Fresnel zone plate and went through a Zernike phase ring and then projected onto a CCD detector to form a projection image.

3. Results and discussion

Figures 2(a) and (b) present amplitude images of the x-ray illumination and the sample, respectively, reconstructed using the iterative method described above. Figure 2(b) was derived

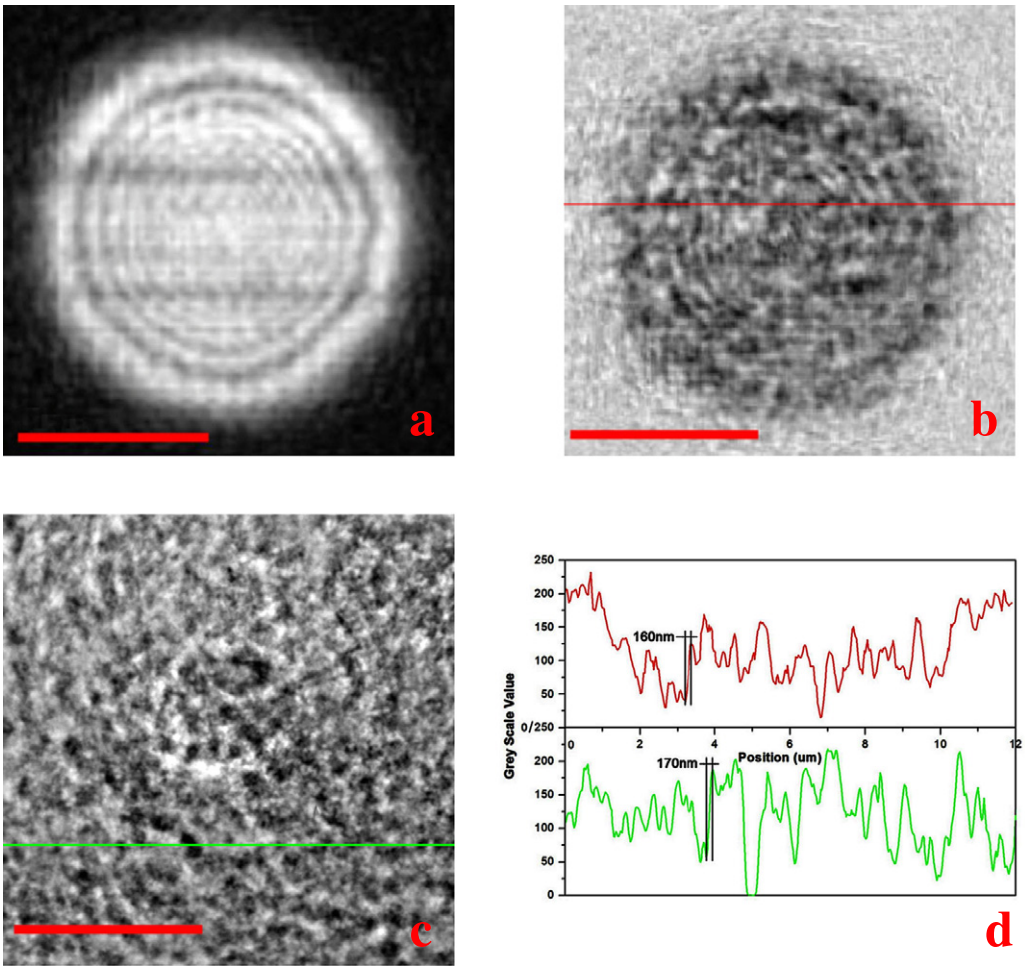

Figure 2. (a) Amplitude image of the illuminating x-ray source (only) reconstructed by the coherent x-ray imaging method. (b) Reconstructed amplitude image of the paint sample. (c) 2D TXM projection of a different region of the same paint sample. (d) Plots of the images along the lines in panels (b) and (c): the upper red curve is the amplitude plot along the red line in panel (b) and the lower green curve is the plot along the green line in panel (c). The scale bars in panels (a)–(c) represent 5 μm.

by dividing the image of the illumination (figure 2(a)) by the image of the sample under illumination. Figure 2(c) is a two-dimensional (2D) projection of a different region of the same sample from the TXM at the beamline 32-ID-C of the APS. The TXM projection is an absorption contrast dominated image. Comparing with figure 2(a), many black dots can be clearly seen in figure 2(b). Similar black dots are obviously observed in figure 2(c) as well. We identify these dots as iron oxide particles. The size of these particles is about 300 nm, which is in good agreement with the size of iron oxide red pigment particles provided by the manufacturer. In figure 2(b), the iron oxide particles are neither homogeneously distributed nor seriously agglomerated in the alkyd resin. A similar distribution of the iron oxide particles can also be observed in figure 2(c). This may cause the cured coating film to have relatively lower UV resistance at some regions and stops it from producing optimal UV resistance.

A recognizable pattern of the illumination beam can be seen in the sample amplitude image (figure 2(b)). This can be attributed to incomplete subtraction of the reconstruction of the illumination beam from that of the sample (with illumination), possibly related to instrument instability between the two measurements.

Introduction of the wave-front modulator is essential for the success of the method, although the choice of phase plate pattern can be somewhat arbitrary, if it can provide sufficient modulation to the x-ray wave-fronts. For instance, a uniformly redundant array pattern plate would work well in the system. The installed phase plate is claimed to be random-patterned because the pixels in the grid are randomly 'filled' with gold or left empty. This type of plate is expected to perform efficiently with all kinds of samples, and is not specifically customized to imaging paint coatings. Employment of the random-patterned phase plate minimizes the correlations among the recorded diffraction patterns and maximizes the retrievable information from single acquisition, because the plate redistributes every object point of the transmitted beam by the specimen to the whole sensing region of the detector. Consequently, the influence of noise and the required dynamic range of the detector are dramatically reduced, which releases us from using a central beam stop and its resulting massive information loss. Furthermore, it helps us to overcome stagnation of the phase retrieval process because the random phase plate effectually breaks possible symmetries in the object field during measurements. As a result, the algorithm converges rapidly and offers the routine a unique solution.

In the imaging system, the resolution of the reconstructed images can be evaluated from the lateral width of the variation of signal from 10 to 90% at the boundaries of features in images [16]. By this criterion, the approximate resolution of the reconstructed amplitude image from our method and the 2D projection from the TXM are both around 120 nm (see figure 2(d)). The achievable resolution of the TXM at 32-ID-C of the APS is 38 nm for the configuration used in this paper [26]. For our method, the resolution is dependent on the detection solid angle and the scattering strength of the sample, which for the present geometry could in principle achieve a similar resolution to the TXM we used. Furthermore, unlike TXMs using Fresnel zone plates, the resolution of the demonstrated coherent x-ray imaging system is not fundamentally limited by the x-ray optical lens.

4. Conclusions

In this paper, we demonstrated a practical coherent x-ray imaging technique that achieved 120 nm spatial resolution using a phase retrieval algorithm by introducing the wave-front modulation to solve the phase problem. It has been demonstrated that this method works well with industrial specimens. In principle, the use of the phase plate modulator provides us a method of producing very-high-resolution images without the disadvantage of the resolution limit imposed by x-ray optics, such as the Fresnel zone plates used in current TXMs. Relative to other coherent diffractive imaging techniques, our method also reduces the requirement for a high dynamic range of the detector. The associated iterative algorithm helps us to overcome stagnation issues that occur in phase retrieval from a single diffraction pattern (e.g. the 'twin' images), and our method also allows us to measure extended samples.

In future, we intend to achieve a larger field of view and a higher spatial resolution. To develop the system into a single-shot x-ray imaging system for extended samples is an important aim of our future work. In the single-shot imaging system [27], multiple phase modulator positions are no longer required and the unique image solution is provided by the reconstruction

done from only a single diffraction pattern. The single-shot x-ray imaging system would be highly suitable for fourth-generation light sources, such as x-ray free electron lasers that are capable of damaging the samples.

Acknowledgments

The work was supported by the Engineering and Physical Sciences Research Council (EPSRC, UK) through a Dorothy Hodgkin Postgraduate Award to BC, a Basic Technology grant ('Ultimate Microscopy', EP/E034055/1), a Phase Modulation Technology for X-ray Imaging grant (EP/I022562/1) and a facility exploitation grant (EP/F020767/1). The coherent x-ray imaging experiment was carried out at the cSAXS beamline at the Swiss Light Source, Paul Scherrer Institut, Villigen PSI, Switzerland. The TXM projection was acquired at beamline 32-ID-C of the APS, which was supported by the US Department of Energy (DOE) under contract no. DE-AC02-06CH11357). RJB acknowledges travel support from the European Community's Seventh Framework Programme (FP7/2007–2013) through grant no. 226716. YSC acknowledges support from the US DOE under contract no. DE-AC-02-98CH1-886.

References

[1] Williams G J, Pfeifer M A, Vartanyants I A and Robinson I K 2003 *Phys. Rev. Lett.* **90** 175501
[2] Shapiro D *et al* 2005 *Proc. Natl Acad. Sci. USA* **102** 15343–46
[3] Chapman H N *et al* 2006 *Nat. Phys.* **2** 839–43
[4] Abbey B, Williams G J, Pfeifer M A, Clark J N, Putkunz C T, Torrance A, McNulty I, Levin T M, Peele A G and Nugent K A 2008 *Appl. Phys. Lett.* **93** 214101
[5] Berenguer de la Cuesta F, Wenger M P E, Bean R J, Bozec L, Horton M A and Robinson I K 2009 *Proc. Natl Acad. Sci. USA* **106** 15297–301
[6] Nishino Y, Takahashi Y, Imamoto N, Ishikawa T and Maeshima K 2009 *Phys. Rev. Lett.* **102** 018101
[7] Dierolf M, Menzel A, Thibault P, Schneider P, Kewish C M, Wepf R, Bunk O and Pfeiffer F 2010 *Nature* **467** 436–9
[8] Miao J, Charalambous P, Kirz J and Sayre D 1999 *Nature* **400** 342–4
[9] Rodenburg J M, Hurst A C, Cullis A G, Dobson B R, Pfeiffer F, Bunk O, David C, Jefimovs K and Johnson I 2007 *Phys. Rev. Lett.* **98** 034801
[10] Abbey B, Nugent K A, Williams G J, Clark J N, Peele A G, Pfeifer M A, Jonge M D and McNulty I 2008 *Nat. Phys.* **4** 394–8
[11] Fienup J R 1982 *Appl. Opt.* **21** 2758–69
[12] Fienup J R and Wackerman C C 1986 *J. Opt. Soc. Am.* A **3** 1897–907
[13] Faulkner H M L and Rodenburg J M 2004 *Phys. Rev. Lett.* **93** 023903
[14] Thibault P, Dierolf M, Bunk O, Menzel A and Pfeiffer F 2009 *Ultramicroscopy* **109** 338–43
[15] Zhang F, Pedrini G and Osten W 2007 *Phys. Rev.* A **75** 043805
[16] Johnson I, Jefimovs K, Bunk O, David C, Dierolf M, Gray J, Renker D and Pfeiffer F 2008 *Phys. Rev. Lett.* **100** 155503
[17] Reddy V A, Sampathkumaran P S and Gedam P H 1986 *Prog. Org. Coat.* **14** 87–97
[18] Burns D T and Doolan K P 2000 *Anal. Chim. Acta* **422** 217–30
[19] Shareef K M A and Yaseen M 1985 *Prog. Org. Coat.* **13** 347–65
[20] Popa M V, Drob P, Vasilescu E, Mirza-Rosca J C, Santana Lopez A, Vasilescu C and Drob S I 2006 *Mater. Chem. Phys.* **100** 296–303
[21] Kumar A, Vemula P K, Ajayan P M and John G 2008 *Nat. Mater.* **7** 236–41
[22] Pospíšil J and Nešpurek S 2000 *Prog. Polym. Sci.* **25** 1261–335

[23] Fienup J R 1997 *Appl. Opt.* **36** 8352–57
[24] Goodman J W 1996 *Introduction to Fourier Optics* 2nd edn (New York: McGraw-Hill) pp 55–8
[25] Gorelick S, Vila-Comamala J, Guzenko V, Mokso R, Stampanoni M and David C 2010 *Microelectron. Eng.* **87** 1052–6
[26] Chu Y S *et al* 2008 *Appl. Phys. Lett.* **92** 103119
[27] Zhang F and Rodenburg J M 2010 *Phys. Rev.* B **82** 121104